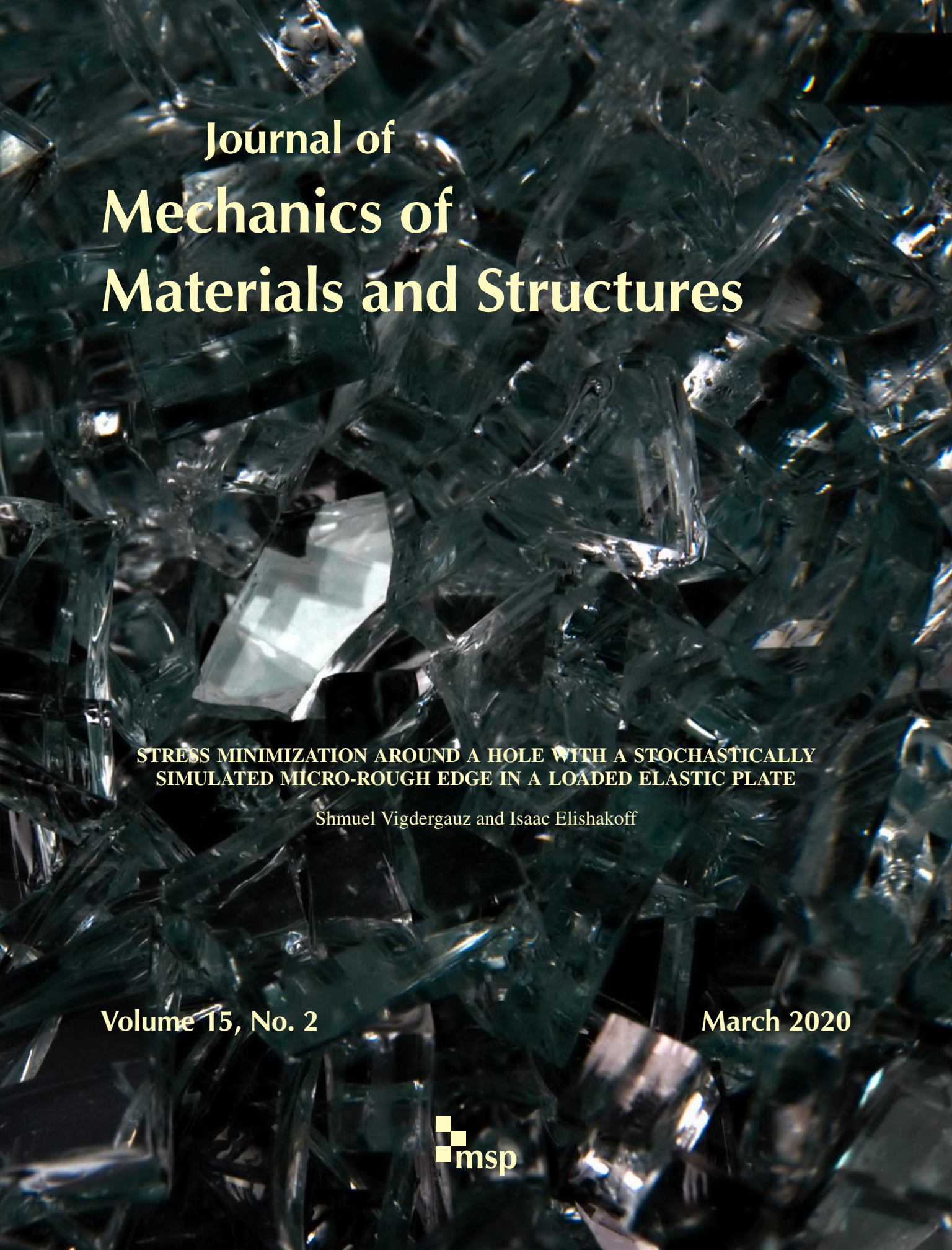

Journal of
Mechanics of
Materials and Structures

STRESS MINIMIZATION AROUND A HOLE WITH A STOCHASTICALLY SIMULATED MICRO-ROUGH EDGE IN A LOADED ELASTIC PLATE

Shmuel Vigdergauz and Isaac Elishakoff

Volume 15, No. 2 March 2020

msp

JOURNAL OF MECHANICS OF MATERIALS AND STRUCTURES
Vol. 15, No. 2, 2020
dx.doi.org/10.2140/jomms.2020.15.277

STRESS MINIMIZATION AROUND A HOLE WITH A STOCHASTICALLY SIMULATED MICRO-ROUGH EDGE IN A LOADED ELASTIC PLATE

SHMUEL VIGDERGAUZ AND ISAAC ELISHAKOFF

A conformal mapping technique is used to simulate a variety of highly oscillating roughness profiles and further to analytically solve the stress field induced around a hole in a thin elastic plate under equi-biaxial tension at infinity. This framework is combined with genetic algorithm scheme to minimize the hoop stress concentration factor (SCF) by appropriately shaping the profile at given integral-type roughness parameters embedded in the optimization as non-linear lower constraints. The effectiveness of the proposed approach is demonstrated by extensive numerical tests aiming to find the SCF-roughness dependence which finally assumes a simple and accurate analytical form applicable in a representative micro-scale range.

1. Background and motivation

Post-machining surface imperfections (roughness) of construction elements are detrimental to their mechanical performance by acting as surface stress concentrators or crack guides. Their adverse effect is conveniently assessed by the stress concentration factor (SCF), defined here as the (dimensionless) ratio between the maximum surface stress and unit applied stresses. Its reliable evaluation is still an open issue, despite significant advances over decades of analytical and numerical studies. For the concerned $2D$ case of flat elements with holes or edges the basic results obtained so far are summarized, for instance, in monographs [Pluvinage 2003; Savruk and Kazberuk 2016].

The key issue here is the arbitrary nature of roughness. One common but not unique approach to stochastically assess the SCF was firstly suggested in [Husu et al. 1975]. As applied to roughness of a single circular hole, it consists of the following steps:

- A close-to-circular hole shape is described in a polar coordinate system (R, θ) as

$$R(\theta) = R_0 + \epsilon H(\theta), \tag{1-1}$$

  where $H(\theta)$, $|H| = O(R_0)$ is a high-oscillating arbitrary function and ϵ is a small parameter used to simulate practically important micro-roughness but, mainly, to simplify the problem's mathematical complexity.

- The dispersions of the Fourier coefficients of $H(\theta)$ are then used to analytically express the ϵ-approximation of the roughness-induced hoop stress as the termwise solution of an ordinary elastostatic problem in two dimensions.

Vigdergauz is the corresponding author.

Keywords: 2D elastostatic problem, Kolosov–Muskhelishvili potentials, stress concentration factor, shape optimization, surface micro-roughness, genetic algorithm.

- Assuming the normal distribution for $H(\theta)$, the "2 standard deviations" rule is finally applied to obtain, with 0.95 certainty, the upper bound on the SCF (displayed in Section 3) as a linear function of two easy-to-measure stochastic parameters of $H(\theta)$. These are: the standard deviation R_{ms} of (zero) mean and the average number n_{cr} of crossing the nominal level per unit length λ, both used as geometrical constraints.

Our aim is to complement this result by numerically finding an attainable (and hence deterministic) lower bound on SCF in the comparable stochastic terms. In other words, we propose to numerically solve the shape optimization problem of finding the SCF-minimizing circular hole with $2\pi/p$-periodic imperfections subject to the above-mentioned roughness factors. Here p is a sufficiently large parameter which serves for simulation of random, highly localized roughness elements.

In the non-stochastic context, a similar approach was effectively used in the authors' previous papers [Vigdergauz 2006; Vigdergauz and Elishakoff 2019] and especially in [Vigdergauz and Elishakoff 2020] where the above-sketched problem was solved at the macroscale, that is under *small* values of p, *large* shape deviations and constraints somewhat differing from (1), (2).

The approach includes three main components:

(1) A finite-term conformal mapping to generate a rapidly oscillating hole shape. This allows us to use the whole methodology of the complex variable techniques and hence to adequately handle complicated biharmonic problems of 2D elastostatics.

(2) An exact direct solver (EDS) for hoop stress along any such shape as developed in [Vigdergauz 2006; Vigdergauz and Elishakoff 2019; 2020].

(3) A standard genetic algorithm (GA) of the global SCF-minimization in a large space of shapes under geometrical constraints which simulate given roughness parameters.

The validity of the proposed scheme was verified by detailed computer simulations results, in which lies the novelty of the study. The results obtained provide the attainable lower bound on the SCF in dependence on the roughness level fitting neatly into a straight line. The particular properties of the SCF-minimizing shapes and stress distributions are also detected and discussed.

The idea (1) of presenting one-dimensional rough profiles in conformal mapping terms is not absolutely new and most likely has been advanced by Damien Vandembroucq [1997b; 1997a]. Our novelty, however, is in embedding this technique into the effective numerical optimization procedure by which the globally SCF-minimizing profiles are found in a wide space of the mapping coefficients serving as the GA design variables. We gave also a special emphasis to detecting the hoop stress distribution along the SCF-minimizing micro-rough profile which expectedly turns out to be stepwise as in the macro-scale case [Vigdergauz and Elishakoff 2020].

This study is organized as follows. Section 2 briefly recalls our previous results about the conformal mapping-based EDS. The most common roughness parameters are disposed in Section 3, suitably for our purposes. Section 4 formulates the corresponding constrained optimization problem. Section 5 covers the GA scheme together with some computational aspects and practical hints. In Section 6 the numerical results presented and analyzed for different values of the governing parameters thus quantifying the minimal possible influence of a given roughness on the SCF. The final remarks are drawn in Section 7.

2. Brief description and overview of EDS

Consider a thin infinite elastic plate S with a single arbitrarily-shaped hole L in the Cartesian complex plane $z = x + iy$. Let the plate be under biaxial stresses P, Q at infinity. By the Kolosov–Muskhelishvili formalism [Muskhelishvili 1975], the induced stresses in the plate are linearly defined through a pair of holomorphic functions (KM potentials) $\Phi_0(z)$, $\Psi_0(z)$, $z \in S + L$

$$\Phi_0(z)=B+\Phi(z),\Psi_0(z)=\Gamma+\Psi(z); \qquad \Phi(z),\ \Psi(z)=O\left(|z|^{-2}\right) \tag{2-1a}$$

$$4B = Q + P,\ 2\Gamma = Q - P \tag{2-1b}$$

In particular, along the hole boundary, the local curvilinear stresses are given as

$$\sigma_{nn}(t)+\sigma_{\tau\tau}(t)=2\left(B+\Phi(t)+\overline{\Phi(t)}\right), \qquad t\in L, \tag{2-2a}$$

$$\sigma_{\tau\tau}(t)-\sigma_{nn}(t)+2i\sigma_{n\tau}=2\frac{dt}{d\bar{t}}\left(\Gamma+\bar{t}\Phi'(t)+\Psi(t)\right). \tag{2-2b}$$

A loading condition along the hole boundary is then obtained by combining (2-2a) and (2-2b)

$$2Re\Phi(t)+B-\frac{dt}{d\bar{t}}\left(\Gamma+\bar{t}\Phi'(t)+\Psi(t)\right)=\sigma_{nn}-i\sigma_{n\tau}. \tag{2-3}$$

Suppose, for concreteness, that the remote loading is isotropic ($Q = P$ and, hence, $\Gamma = 0$) while the piecewise-smooth hole boundary L is traction-free ($\sigma_{nn}, \sigma_{n\tau} = 0$). Then in view of (2-1b), (2-2a) we have

$$\mathcal{K}=\frac{\max|\sigma_{\tau\tau}(t)|}{P}=2\frac{\max|B+\mathrm{Re}\,\Phi(t)|}{B}, \quad t\in L, \tag{2-4}$$

where $\mathcal{K}$ denotes the SCF.

Specifically, for an ideal circle $\gamma : |t| = R_0, \bar{t} = t^{-1}$ the solution of the boundary value problem (2-3) for $\Phi(z)$, $\Psi(z)$ with the asymptotics (2-1) simplifies to (see [Muskhelishvili 1975])

$$\Phi_0(z)=B,\ \ \Psi_0(z)=\Psi(z)=2BR_0^2z^{-2}, \qquad z\in S+\gamma, \tag{2-5}$$

and therefore, with (2-2),(2-3)

$$\sigma_{\tau\tau}(t)=\mathrm{Const}=2P,\ \ t\in\gamma \quad \Rightarrow \quad \mathcal{K}=2. \tag{2-6}$$

The SCF definition (2-4) supposes implicitly that the hole shape has no angular points and cusps where the hoop stress may be infinite. This circumstance, however, is not limiting in the current context of stress minimization, which makes such points irrelevant.

The analytical framework (2-1)–(2-4) can be generalized by conformal mapping $\omega(\zeta)$ of the γ exterior $\Sigma : |\zeta| \geq R_0$ onto the exterior of an arbitrary hole shape L with correspondence of the boundaries and the points at infinity [Muskhelishvili 1975]

$$\Sigma+\gamma \xrightarrow[\omega(\zeta)]{} S+L, \qquad \omega(\zeta)=R_0\zeta+O(|\zeta|^{-1}). \tag{2-7}$$

In order to model the boundary roughness by a periodic topography, let us suppose that the holomorphic function $\omega(\zeta)$, and hence the mapped shape L, possess p-fold rotational symmetry about the origin:

$$\omega(e^{i\beta}\zeta)=e^{i\beta}\omega(\zeta), \qquad \beta=2\pi/p, \tag{2-8}$$

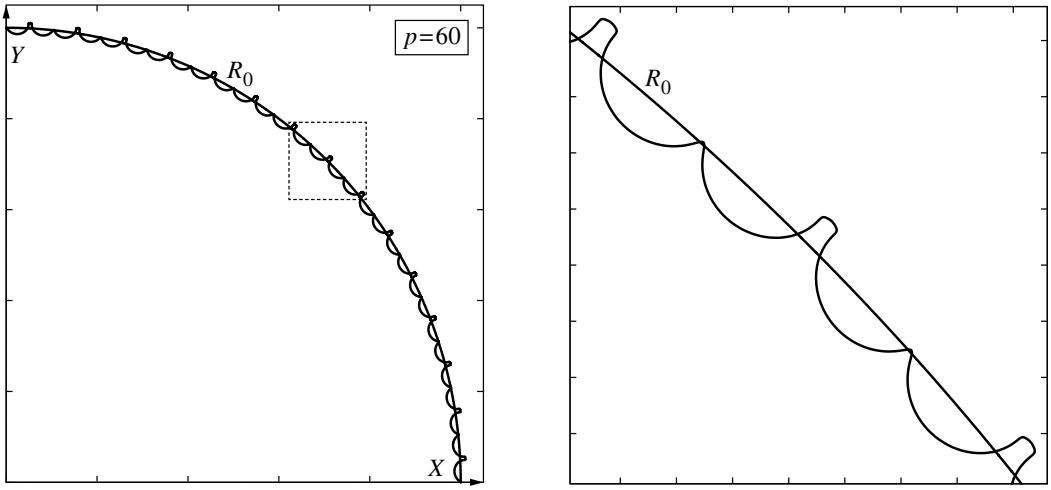

Figure 1. Surface roughness simulation. A multi-wavy hole shape (left) conformally mapped via $\omega(\xi)$ at $M = 5$ and $p = 60$. An enlarged view of the dotted square is given on the right.

as exemplified in Figure 1 for $p = 60$. Consequently, for an isotropic load $P = Q$, [Muskhelishvili 1975]

$$\Phi(e^{i\beta}\zeta) = \Phi(\zeta), \qquad \Psi(e^{i\beta}\zeta) = e^{-2i\beta}\Psi(\zeta), \tag{2-9}$$

or, equivalently, in terms of Laurent series in $\Sigma + \gamma$,

$$\omega(\zeta) = R_0\zeta + \sum_{k=1}^{\infty} \frac{d_k}{\zeta^{kp-1}}, \quad \Phi(\zeta) = \sum_{k=1}^{\infty} \frac{a_k}{\zeta^{kp}}, \quad \Psi(\zeta) = \sum_{k=1}^{\infty} \frac{b_k}{\zeta^{kp+2}}, \tag{2-10}$$

where $\Phi(\zeta)$, $\Psi(\zeta)$ are the KM potentials transformed to variable ζ. In view of loading symmetry all the coefficients in (2-10) can be taken as real-valued quantities without loss of generality.

Note that the boundary hoop stresses $\sigma_{\tau\tau}(t)$ in (2-2a) are expressed by only $\Phi(\zeta)$. At given L, this permits to solve the potentials in tandem rather than in parallel, thus halving the computational cost of finding $\mathcal{K}$ [Kalandia 1975]. Indeed, substitution of (2-10) into the specially prearranged boundary condition (2-2b) followed by equating the coefficients of like powers of ζ yields an infinite system $\mathcal{H}$ of linear algebraic equations in the unknowns $\{a_k\}$ with real matrix elements composed of $\{d_k\}$ and integers. They are not displayed here to save room. For full details see [Vigdergauz 2006; Vigdergauz and Elishakoff 2019].

In numerical practice the infinite expansion (2-10) for $\omega(\zeta)$ is commonly truncated to the first M terms: $d_k = 0$, $k > M$ (though both other series remain *infinite*). This is justified in the current context since the $\mathcal{K}$-minimization tends to smooth local shape curvatures mainly being formed by higher Laurent coefficients.

In particular, the sawtooth-like surface displayed in Figure 1 is obtained at $M = 8$. To avoid confusion, note that this is *not* the SCF-minimizing shape, and consequently it exhibits large (but finite) local curvatures to be smoothed as much as possible in further optimization.

Remarkably, this finite approximation decomposes the initial system $\mathcal{H}$ into two subsystems - (a) the first M non-vanishing equations for the first M non-zero unknowns $\{a_k\}$ and (b) the infinite remainder for the "tail" $\{a_k\}$, $k > M$. The key feature of the subsystem (b) is its finite-differences structure [Levi and Lessman 1992] by which the "tail" is expressed *analytically* through the first M unknowns as proved at length in [Vigdergauz 2006; Vigdergauz and Elishakoff 2019]. The resulting formula reads

$$\Phi(\xi) = \frac{R_M(\bar{\xi})}{\xi\omega'(\xi)}, \qquad \xi \in \gamma, \tag{2-11}$$

where $R_M(\xi)$ is a polynomial of degree M in ξ

$$R_M(\xi) = r_M\xi^M + r_{M-1}\xi^{M-1} + \cdots + r_0, \tag{2-12}$$

with coefficients

$$r_0 = a_1 = 0, \quad r_1 = a_2, \quad r_m = a_{m+1} - \sum_{k=2}^{m} (-1)^k k d_k a_{m+k+1}, \quad m \geq 2. \tag{2-13}$$

In other words, Equations ((2-11)–(2-13)) are *exact* up to negligible errors caused by numerically solving the subsystem (a) at moderate values of M. Note that just this (almost) analytical solution of the direct problem within the GA process provides the numerical effectiveness of the SCF optimization in bounded M-dimensional searching space Π_M of the design variables $\{d_1, d_2, \ldots, d_M\}$ all of them being restricted within the successfully narrowing intervals

$$-\frac{1}{\sqrt{kp-1}} \leq d_k \leq \frac{1}{\sqrt{kp-1}}, \qquad k = 1, 2, \ldots, M, \tag{2-14}$$

which form the necessary (but no means sufficient) condition for the $(L \Leftrightarrow \gamma)$ mapping uniqueness. In the $\mathcal{K}$-minimization context, they are treated as two-sided linear constraints to be imposed together with preset values of roughness parameters. The latter are described and discussed in the next section.

Before continuing, two useful remarks are in order:

First, note that any non-trivial conformal mapping (2-7) always diminishes the area F of L, compared to the unit circle [Ahlfors 1979].

$$0 \leq F(L) = \pi R_0^2 \left(1 - \sum_{k=1}^{M} (kp-1) d_k^2\right) \leq \pi R_0^2 = F(\gamma) \tag{2-15}$$

as clearly seen in Figure 1 (right).

Second, some numerical comparisons [Vigdergauz 2006] show that the error caused by neglecting the exact summation in the infinite subsystem (b) can run to several percents of the $\mathcal{K}$ value and its location. This is significantly worse than accuracy and stability performance routinely achieved even in standard GA schemes.

3. Shape roughness parameters

In the considered 2D case of a perforated thin plate, the machine-induced roughness is treated as the repetitive or random small-scale deviations of a real profile from the ideal geometrical line. These form a one-dimensional, continuous and one-valued surface topography as sketched in Figure 2.

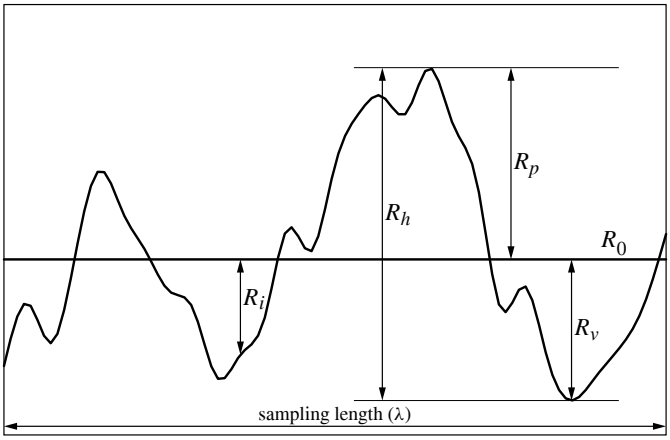

Figure 2. Surface micro-roughness scheme. Note that due to the supposed shortness of the sampling length the circle segment R_0 seems straight with no visible curvature.

Since the sample length λ is very small as compared to R_0 the base-line curvature is unnoticeable within a small angle θ_λ: $R_0\theta_\lambda = \lambda$.

Table 1 presents commonly accepted roughness parameters based on quantifying the peaks, valleys, slopes and crossing certain thresholds [Whitehouse 2012; Thomas 1999] grouped by their geometrical meanings. Here, in notations of (1-1), $H_i = H(\theta_i)$, $H_i' = H'(\theta_i)$, $\theta_i \in [0; \theta_\lambda]$.

A reliable SCF assessment is conventionally based on coupling parameters from both groups. For instance, the probabilistically obtained result from [Husu et al. 1975] mentioned in Section 1 takes the form

$$\mathcal{K} = 2(1+\alpha), \quad \alpha = 8\pi n_{\rm cr} R_{\rm ms}. \tag{3-1}$$

	Amplitude parameters	
R_a	Arithmetical mean deviation from the circle $R = R_0$	$R_a = \dfrac{\epsilon}{n}\sum\limits_{i=0}^{n} \lvert H_i \rvert$
$R_{\rm ms}$	Root mean squared	$R_{\rm ms} = \epsilon\Big(\dfrac{1}{n-1}\sum\limits_{i=0}^{n} H_i^2\Big)^{\frac{1}{2}}$
R_p	Maximum peak height	$R_p = \epsilon \max_i H_i$
R_v	Maximum valley depth	$R_v = \epsilon \min_i H_i$
R_h	Maximum peak-to-valley height	$R_p - R_v$
	Slope and counting parameters	
$n_{\rm cr}$	Average number of crossing the R_0-profile per sample length λ	
n_{pd}	Peaks density: average number of peaks per sample length λ	
$R_{\rm da}$	Arithmetical mean slope of the profile	$R_{\rm da} = \dfrac{\epsilon}{n}\sum\limits_{i=0}^{n} \lvert H_i' \rvert$

Table 1. Surface roughness parameters.

The amplitude parameters are partially interrelated by evident inequalities:

$$R_p \geq R_{\mathrm{ms}} \geq R_a. \tag{3-2}$$

Less trivial *intergroup* relations can be derived for the mean slope R_{da} which is alternatively evaluated [Vigdergauz and Elishakoff 2020] by variation V of $R(\theta)$ on λ. In accordance with the theory of real-valued functions [Natanson 1956] it is here defined through the non-negative discrete sums of absolute values of the differences of $\Delta_i R(\theta) = \Delta_i H(\theta)$ in two adjacent points on λ

$$V[R] = \epsilon V[H] = \epsilon \sup \sum_{i=0}^{n} |H_{i+1} - H_i| \geq 0. \tag{3-3}$$

The supremum is taken over all possible partitions of λ with an arbitrary set of $(n+1)$ points ordered by a chosen direction of traversing. Apparently, only one such set is used in numerically evaluating the variations.

The variations are bounded below [Natanson 1956] as follows (see Table 1 for notation):

$$\epsilon V[H] \geq R_p - R_v = R_h, \tag{3-4}$$

where the equals sign is only true for monotonic functions on λ.

For a differentiable function, we have equivalently to (3-3)

$$V[R] = \epsilon V[H] = \epsilon \int_0^{\theta_\lambda} |H'(\theta)| d\theta = \theta_\lambda R_{\mathrm{da}}. \tag{3-5}$$

Therefore, in view of (3-4) the average slope R_{da} of the profile is bounded below by a ratio of two small numbers:

$$R_{\mathrm{da}} \geq \frac{R_h}{\theta_\lambda}, \tag{3-6}$$

and hence may be arbitrarily large. Since notch steep slopes are known as stress concentrators this potentially invalidates the traditional epsilon-approximation which supposes, either explicitly or implicitly, that R_{ds} and R_h are of the same smallness order; see, for instance, [Pal'mov 1963; Givoli and Elishakoff 1992; Medina and Hinderliter 2014]. A much more elaborate analysis is conducted in the recent papers [Vandembroucq and Roux 1997a; 1997b], where a special iterative algorithm is proposed to deal with large slopes: $R_{\mathrm{da}} = O(1)$.

At this point we note, for clarity, that our scheme is free of the epsilon-expansion shortcomings. The smallness of the amplitude roughness parameters is implied only at the computation stage for obtaining numerical results in the most practical microscale case. Clearly, for fixed, arbitrarily small amplitudes the average slope of the mapped profile grows with increasing rotational symmetry factor p which thus belongs to the group of slope and counting parameters.

On the other hand the SCF minimization expectedly tends to diminish the slope R_{da} as far as possible. Some explanatory numerical examples are given in Section 6.

We also note in advance that, similarly to the macroscale case [Vigdergauz and Elishakoff 2020], the SCF-minimizing profile $R(\theta)$ appears to be monotonic (but not convex) on λ thus saturating the

inequalities in (3-4) and (3-6) and resulting in the identity

$$n_{\mathrm{cr}} = 2n_{pd} = \frac{p}{\pi R_0}, \tag{3-7}$$

which holds because function $R(\theta)$ has no local extrema.

Inasmuch as the amplitude parameters are measured in length units (micrometers or microinches) the normalized multiplier R_0 must appear in any assessment of the scale-independent SCF.

4. Problem formulation: one-sided constraints

The frequency-type parameter p should be further coupled with a certain amplitude parameter to govern the SCF-minimization process and obtain more reliable solutions. For the macroscale case it was the maximum peak-to-valley height R_h [Vigdergauz and Elishakoff 2020], but here we take R_{ms} instead. The argument in favor is that R_{ms} is computationally much more stable, especially at large values of p as in the current case. Additionally, this allows us to obtain the SCF lower bound in terms of upper one (3-1).

Our aim is to numerically minimize the SCF at given p and normalized

$$R_{\mathrm{nms}} = \frac{R_{\mathrm{ms}}}{R_0}, \tag{4-1}$$

in a representative interval of their values. It is significant that these two enter the GA scheme quite differently. While p is fixed at once for the whole search, R_{nms} is computed separately for each generated profile. For this reason it is desirable to keep a preset value R^*_{nms} with a one-sided inequality constraint

$$R_{\mathrm{nms}} \geq R^*_{\mathrm{nms}} > 0, \tag{4-2}$$

which forces genetic algorithm to search for the SCF minimum closest to the level $R_{\mathrm{nms}} = R^*_{\mathrm{nms}}$ providing $\mathcal{K}(R_{\mathrm{nms}})$ monotonically increases with R_{nms}. This intuitively correct presumption is *a posteriori* justified by the numerical results obtained for a dense set of values on the representative microscale interval of R_{nms} as witnessed in Section 6

With these preliminaries, we are now in a position to precisely formulate the following shape optimization problem with the roughness modelling parameters:

Given the external loading type, find, over all admissible set of the design variables $\{d_m, m \leq M\}$*, the* p*-symmetrical hole shape* $L_p \in \Pi_M$ *that minimizes the stress concentration factor* $\mathcal{K}$ *under constraint* (4-2)*:*

$$\mathcal{K}(L_p, M, R^*_{\mathrm{nms}}) \xrightarrow[\{d_m\}]{} \min(p, M, R^*_{\mathrm{nms}}). \tag{4-3}$$

5. GA-based optimization scheme

As already noted in Section 2, it is reasonable to expect a stable solution of (4-3) at modest values of M (typically at most 6 or 8). Such smal-size minimization problem with a single time-consuming objective function are well suited for solving by a genetic algorithm (GA) approach (see, for instance, [Goldberg and Sastry 2010; Kramer 2017]). It mimics the biological principle of "survival of the fittest" underlying natural selection to find the best solution for a specific problem.

Standard GA begins with a randomly generated initial population of possible solutions (individuals) with design variables encoded in ordered binary strings (chromosomes). An individual's fitness is calculated by the EDS (2-11)–(2-13) and (2-4) and some of them are selected as parents according to their fitness values. A new population (children) is produced by applying the bit-wise crossover operator to the parents and then applying the bit-wise mutation operator to their offsprings. The iterations involving the replacement of the original parent's generation with a children's one are repeated until the stopping criterion is satisfied.

Before evaluating the fitness each binary string must be decoded to a certain ordered sequence $\{d_k\}$ within the intervals (2-14). However, in doing so, self-intersecting (multiple valued) shapes may appear, since. as noted in Section 2, these inequalities are not sufficient to guarantee their absence.

Unfortunatly, no conditions in $\{d_k\}$ terms to detect self-intersections are known thus far. Therefore, we check each decoded curve for possibly breaking the monotonicity,

$$\frac{d \arg \omega(\theta)}{d\theta} \geq 0, \quad \theta \in [0; \theta_\lambda] \quad \theta_\lambda = \frac{\pi}{p}, \tag{5-1}$$

which provides the more restrictive shape property of star-shapeness because, physically, only star-shaped holes are really promising for optimization. In the numerical simulations this is confirmed by that the optimal values of $\{d_m\}$ are rather distant from the intervals limiting values (2-14).

After decoding each string into the corresponding shape its fitness $\mathcal{K}$ is then computed through (2-11) - (2-13) at a large number of points. Whenever the current shape violates either of the imposed constraints (4-2), (5-1), a significant constant penalty is assigned as its fitness value without further computation of $\mathcal{K}$.

Finally, it is important to note that while all other steps of a GA are well defined, there are few theoretical guidelines for determining when to terminate the search. Though the use of a global scheme rather than a gradient-type scheme is intended to avoid being trapped in local optima, this does occur especially for large (up to 4500) values of p required in the considered microscale case. The question is which number of fitness function evaluations (or number of iterations) is needed o find the global optimum with a high certainty. Several semi-heuristic stopping criteria are proposed thus far (see the survey by [Ghoreishi et al. 2017]). Especially relevant here is the N-criterion [Leung and Wang 2001; Bhandari et al. 2012] which is fulfilled if there is no improvement in the best fitness values through N consecutive iterations. For better confidence in the results we took $N = 100$ and performed up to five independent runs at each computational point making the process more time-consuming than in the macroscale case [Vigdergauz and Elishakoff 2020] with $p = 4$.

6. Numerical results

. Our final aim is to find an accurate analytical approximation for $\alpha(p, R_{\text{nms}})$ using its values computed for a representative number of discrete points within pre-specified intervals $[p^{min}; p^{\max}]$, $(0; R^{\max}_{\text{nms}}]$. These should be chosen in accordance with the micro-rougness ISO grade numbers N_{grade} and reasonable computational efforts. We take $p^{min} = 900$, $p^{\max} = 4500$, $R^{\max}_{\text{nms}} = 0.0002$. This covers several N_{grade} in dependence on the hole neutral radius R_0.

Preparatory to obtaining the main result of this Section, we analyze $\alpha(p, R_{\text{nms}})$ individually for either (of the two) parameter at fixed values of the second one as presented in Figure 3, which suggests a close to linear behavior in the chosen intervals.

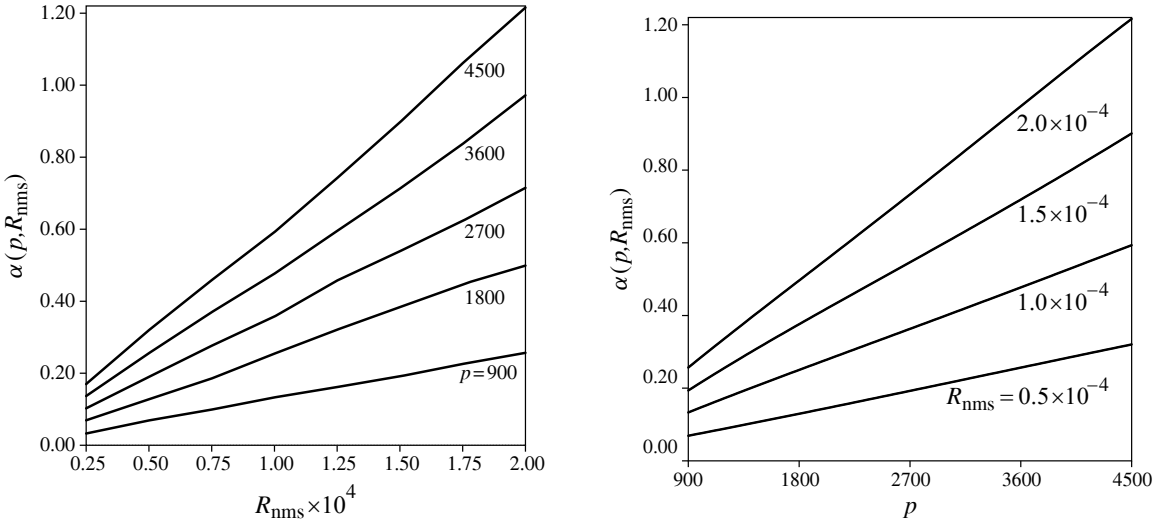

Figure 3. Coefficient $\alpha(p, R_{\rm nms})$ at several fixed values of p (left) and $R_{\rm nms}$ (right) in dependence on the complementary parameter.

In view of this the aggregated dependence $\alpha(pR_{\rm nms})$ on the parameters product has been computed with much higher resolution (Figure 4). It is seen that the computed data fit neatly the linear least square (LLS) approximation

$$\alpha = 1.337 pR_{\rm nms}, \tag{6-1}$$

with the normalized root-mean-square deviation 0.4%.

Next, substitution of (3-7) into (6-1) gives in the convenient roughness parameters

$$\alpha = 1.337\pi n_{\rm cr} R_{\rm ms}. \tag{6-2}$$

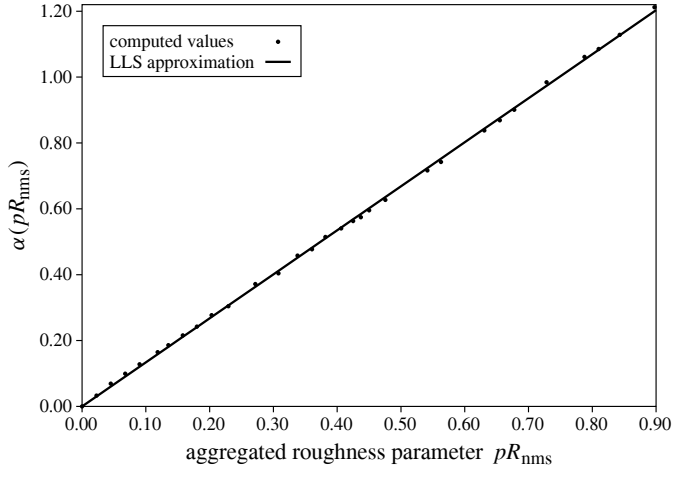

Figure 4. Variations of the coefficient α with the aggregated roughness parameter $pR_{\rm nms}$.

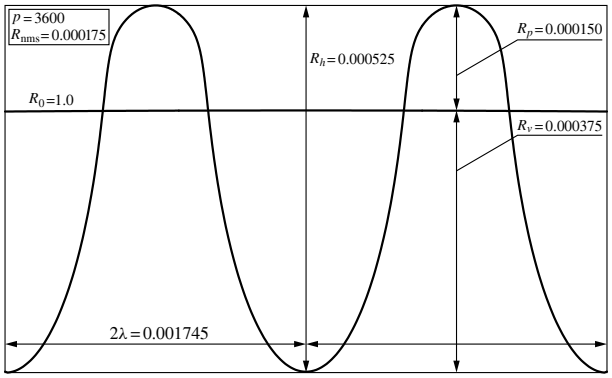

Figure 5. Typically smoothed notches of the $\mathcal{K}$-optimal hole shape.

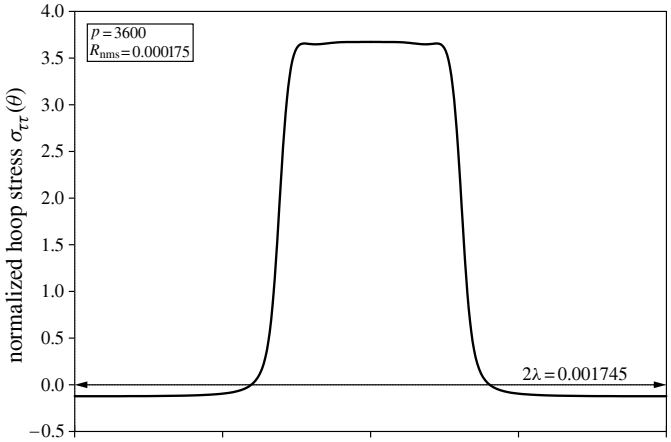

Figure 6. Typical stepwise stress distribution along the $\mathcal{K}$-optimal notch.

Taken together, (3-1) and (6-2) form a two-side interval

$$\alpha \in [1.337;\, 8]\pi n_{\rm cr} R_{\rm ms}. \tag{6-3}$$

We note again that in contrast to the deterministic lower bound the upper one is of stochastic nature with the 95% confidence.

A typical $\mathcal{K}$-minimizing roughness profile is exemplified in Figure 5 together with the resultant values of the amplitude roughness parameters.

Expectedly, the SCF-minimization forms strongly-smoothed notches in order to avoid local stress concentrators associated with large curvatures along the profile. Quantitatively, this observation is supported by the fact that the optimal shape $R(\theta)$ is ivariably monotonic om λ thus providing the minimum (3-6) of the avrage notch slope $R_{\rm da}$. Particularly, for the data displayed in Figure 5 ($p = 3600$, $R_{\rm nms} = 0.000175$) we have $R_{\rm da} \approx 0.60$ which is far from being ϵ-small. For $p = 4500$ and $R_{\rm nms} = 0.0002$, $R_{\rm da}$ increases up to ≈ 0.82.

Figure 6 depicts a typical stress distribution along the $\mathcal{K}$ optimal notch. This stepwise pattern is an extension of the equi-stress (constant) distribution to the optimal shapes under geometric constraint, as was first found in [Vigdergauz 2013].

7. Concluding remarks

Our previous technique of minimizing the elastic SCF induced by a given circular surface roughness at the macrolevel [Vigdergauz and Elishakoff 2020] has been extended here to microscale asperities whose stochastic distribution is realized deterministically through a finite-term conformal mapping as a rapidly oscillating periodic profile. This representation pursues two constructive outcomes. First, a fast and (almost) exact $2D$ direct solver with no epsilon-approximation is developed and embedded into the GA scheme. Second, given roughness measures are easily computed and controlled as efficient lower constraints on the minimized SCF. As a result a (previously unknown) attainable lower bound on the SCF is obtained in dependence on two commonly used engineering parameters of surface topography. Additionally, it was also found that the $\mathcal{K}$-optimal hole shape forms a single smooth notch with the possibly minimal average slope of its edges and a step-wise stress distribution.

References

[Ahlfors 1979] L. Ahlfors, *Complex analysis*, 3rd ed., McGraw-Hill, New York, 1979.

[Bhandari et al. 2012] D. Bhandari, C. A. Murthy, and S. K. Pal, "Variance as a stopping criterion for genetic algorithms with elitist model", *Fundam. Inf.* **120**:2 (2012), 145–164.

[Ghoreishi et al. 2017] S. Ghoreishi, A. Clausen, and B. Joergensen, "Termination criteria in evolutionary algorithms: a survey", pp. 373–384 in *Proceedings of the 9th International Joint Conference on Computational Intelligence*, vol. 1, SciTePress, 2017.

[Givoli and Elishakoff 1992] D. Givoli and I. Elishakoff, "Stress concentration at a nearly circular hole with uncertain irregularities", *J. Appl. Mech.* (*ASME*) **59**:2S (1992), S65–S71.

[Goldberg and Sastry 2010] D. Goldberg and K. Sastry, *Genetic algorithms: the design of innovation*, Springer, 2010.

[Husu et al. 1975] F. P. Husu, Y. R. Vitenberg, and V. A. Pal'mov, Шероховатость поверхностей: теоретико-вероятностный подход, Nauka, Moscow, 1975.

[Kalandia 1975] A. I. Kalandia, *Mathematical methods of two-dimensional elasticity*, Mir, Moscow, 1975.

[Kramer 2017] O. Kramer, *Genetic algorithm essentials*, Springer, 2017.

[Leung and Wang 2001] Y. Leung and Y. Wang, "An orthogonal genetic algorithm with quantization for global numerical optimization", *Trans. Evol. Comp* **5**:1 (2001), 41–53.

[Levi and Lessman 1992] H. Levi and F. Lessman, *Finite difference equations*, Dover, New York, 1992.

[Medina and Hinderliter 2014] A. Medina and B. Hinderliter, "The stress concentration factor for slightly roughened random surfaces: Analytical solution", *Int. J. Solids Struct.* **51**:10 (2014), 2012–2018.

[Muskhelishvili 1975] N. I. Muskhelishvili, *Some basic problems of the mathematical theory of elasticity*, second ed., Noordhoff, Leiden, 1975.

[Natanson 1956] I. P. Natanson, *Theory of functions of a real variable*, Ungar, New York, 1956.

[Pal'mov 1963] V. A. Pal'mov, "Stress state in vicinity of irregular surfaces of elastic bodies", *Prikl. Mat. Mekh.* 5 (1963). In Russian.

[Pluvinage 2003] G. Pluvinage, *Fracture and fatigue emanating from stress concentrators*, Springer, 2003.

[Savruk and Kazberuk 2016] M. P. Savruk and A. Kazberuk, *Stress concentration at notches*, Springer, 2016.

[Thomas 1999] T. R. Thomas (editor), *Rough surfaces*, 2nd ed., Imperial College Press, London, 1999.

[Vandembroucq and Roux 1997a] D. Vandembroucq and S. Roux, "Conformal mapping on rough boundaries, I: Applications to harmonic problems", *Phys. Rev. E* **55**:5 (1997), 6171–6185.

[Vandembroucq and Roux 1997b] D. Vandembroucq and S. Roux, "Conformal mapping on rough boundaries, II: Applications to biharmonic problems", *Phys. Rev. E* **55**:5 (1997), 6186–6196.

[Vigdergauz 2006] S. Vigdergauz, "Stress-minimizing hole in elastic plate under remote shear", *J. Mech. Mater. Struct.* **1**:2 (2006), 387–406.

[Vigdergauz 2013] S. Vigdergauz, "A generalization of the equi-stress principle in optimizing the mechanical performance of two-dimensional grained composites", *Math. Mech. Solids* **18**:4 (2013), 431–445.

[Vigdergauz and Elishakoff 2019] S. Vigdergauz and I. Elishakoff, "Energy-maximizing holes in an elastic plate under remote loading", *J. Mech. Mater. Struct.* **14**:1 (2019), 139–154.

[Vigdergauz and Elishakoff 2020] S. Vigdergauz and I. Elishakoff, "Stress-minimizing holes with a given surface roughness in a remotely loaded elastic plane", *J. Mech. Mater. Struct.* **15**:1 (2020), 1–14.

[Whitehouse 2012] D. J. Whitehouse, *Surfaces and their measurement*, second ed., Butterworth-Heinemann, 2012.

Received 3 Mar 2020. Revised 12 Mar 2020. Accepted 19 Mar 2020.

SHMUEL VIGDERGAUZ: shmuelvigdergauz@gmail.com
Research and Development Division, The Israel Electric Corporation Ltd., Haifa, Israel

ISAAC ELISHAKOFF: elishako@fau.edu
Department of Ocean and Mechanical Engineering, Florida Atlantic University, Boca Raton, FL, United States

JOURNAL OF MECHANICS OF MATERIALS AND STRUCTURES

msp.org/jomms

Founded by Charles R. Steele and Marie-Louise Steele

Cover photo: Mando Gomez, www.mandolux.com

See msp.org/jomms for submission guidelines.

JoMMS (ISSN 1559-3959) at Mathematical Sciences Publishers, 798 Evans Hall #6840, c/o University of California, Berkeley, CA 94720-3840, is published in 10 issues a year. The subscription price for 2020 is US $660/year for the electronic version, and $830/year (+$60, if shipping outside the US) for print and electronic. Subscriptions, requests for back issues, and changes of address should be sent to MSP.

JoMMS peer-review and production is managed by EditFLOW® from Mathematical Sciences Publishers.

PUBLISHED BY

mathematical sciences publishers

nonprofit scientific publishing

http://msp.org/

Journal of Mechanics of Materials and Structures

Volume 15, No. 2 March 2020

1559-3959(2020)15:2;1-K